

Photodissociation Spectroscopy of Benzene Cluster Ions in Ultraviolet and Infrared Regions. Static and Dynamic Behavior of Positive Charge in Cluster Ions

Yoshiya Inokuchi and Nobuyuki Nishi*

Institute for Molecular Science, Myodaiji, Okazaki 444-8585, Japan

Photodissociation spectroscopy is applied to benzene cluster ions in ultraviolet and infrared regions. In the ultraviolet photodissociation spectrum of $(\text{C}_6\text{H}_6)_3^+$, a characteristic broad band emerges at 255 nm. This band is assigned to a $\pi^* \leftarrow \pi$ transition of a solvent benzene molecule that exists in the trimer. This is in accord with the previous model of the ion cluster with a dimer ion core and a solvent benzene molecule. The infrared photodissociation spectra of $(\text{C}_6\text{H}_6)_n^+$ ($n=3-5$) show a sharp band at 3066 cm^{-1} . The band is attributed to a C–H stretching vibration of the dimer ion core. The infrared spectra of $(\text{C}_6\text{H}_6)_n^+$ ($n=3-5$) are fitted to the model spectra reproduced by combining the C–H stretching bands of the dimer ion core and the solvent benzene molecule. The infrared photodissociation spectra of mixed benzene trimer ions with one or two benzene- d_6 molecules demonstrate that there is no correlation between the excited dimer ion core site in the trimer and the photofragment dimer ion species. This implies that a dimer ion core switching occurs in photoexcited vibrational states prior to the dissociation.

* Author to whom all correspondence should be addressed; e-mail: nishi@ims.ac.jp

I. INTRODUCTION

In the last decade, we have studied the photodissociation spectroscopy and the photodissociation dynamics of benzene cluster ions, $(\text{C}_6\text{H}_6)_n^+$.¹⁻³ In the photodissociation spectrum of $(\text{C}_6\text{H}_6)_2^+$ in the near-infrared region, two strong absorption bands are seen at 915 nm and 1155 nm.¹ These are assigned to the charge resonance bands. The charge resonance band is due to the transition from the ground state to the repulsive excited state of the wave functions,¹

$$\psi_+ = (2+2S)^{-1/2}(\psi_1^+\psi_2 + \psi_1\psi_2^+); \quad (1a)$$

$$\psi_- = (2-2S)^{-1/2}(\psi_1^+\psi_2 - \psi_1\psi_2^+), \quad (1b)$$

respectively. ψ_i^+ and ψ_i ($i=1, 2$) are the electronic wave functions of $\text{C}_6\text{H}_6^+(\text{X})$ and $\text{C}_6\text{H}_6(\text{X})$, respectively, and $S = \langle \psi_1^+\psi_2 | \psi_1\psi_2^+ \rangle$. The presence of the charge resonance band implies that the two moieties should be equivalent to each other, and that the positive charge is delocalized in the dimer. In mass-selected photodepletion spectra of $(\text{C}_6\text{H}_6)_n^+$ ($n = 3-6$) in the range of 800–1100 nm,² the absorption bands exhibit essentially the same features as observed for $(\text{C}_6\text{H}_6)_2^+$. This little change in the electronic spectra suggests the presence of a dimer ion core in the clusters. We also studied excess energy partitioning in the photodissociation process of $(\text{C}_6\text{H}_6)_n^+$, and concluded that the intramolecular vibrations of the ejected neutral monomers are highly excited in the energy disposal.^{2, 3} If the charge continually hops in the cluster after the photoexcitation, the ejected molecules should be vibrationally excited along the directions of the change in the equilibrium geometries between the neutral and the ion.

In this paper, we discuss both static distribution of the positive charge in the

electronic ground state and dynamic charge hopping in the photoexcited states of benzene cluster ions. First, a photodissociation spectrum of benzene trimer ion in the ultraviolet region is presented, where one can see an electronic transition assignable to a solvent benzene molecule. The spectrum supports the dimer ion core structure with one solvent benzene molecule in the trimer ion. We also display photodissociation spectra of benzene cluster ions in the infrared region. Vibrational transitions of the dimer ion core and the solvent molecules are reported. Finally, we demonstrate a dimer ion core switching in photoexcited vibrational states by showing photodissociation spectra of isotopically mixed benzene trimer ions that contain one or two benzene- d_6 molecules.

II. EXPERIMENT

The photodissociation spectra of benzene cluster ions are measured by using an ion guide spectrometer with two quadrupole mass filters.⁴ Mixture of benzene, benzene- d_6 , and argon is expanded into a vacuum chamber through a pulsed nozzle (General Valve Series 9) with a 0.80 mm orifice diameter and a 300 μ s pulse duration. The total stagnation pressure is 2×10^5 Pa in most cases, and the benzene content in the mixture is 4%. Neutral benzene clusters are ionized by a home-made electron-impact ionizer situated near the exit of the pulsed nozzle. Electron kinetic energy is adjusted to 350 eV. Temperatures of benzene cluster ions were estimated to be 80–120 K.⁵ After passing through a skimmer, benzene cluster ions are introduced into the spectrometer, and the parent ions are isolated by the quadrupole mass filter. After the deflection by 90° through an ion bender,⁶ the ion beam is decelerated and introduced into the quadrupole ion guide. The ion beam is merged with a laser beam in the ion guide. Photoexcitation induces fragmentation of the parent ions. After the second deflection at an angle of 90° by another ion bender, fragment ions are mass-selected through the quadrupole filter, and detected by a microsphere plate (El-Mul Technologies). For the normalization of yield spectra, the power of the dissociation laser is monitored by a pyroelectric detector (Molelectron P1-15H-CC). Both the ion signals from the microsphere plate and the laser signals from the pyroelectric detector are fed into a digital storage oscilloscope (LeCroy 9314A). The oscilloscope is controlled by a microcomputer through a GPIB interface. Photodissociation spectra of the parent ions are obtained by plotting the normalized yields of the fragment ions

against the wavelengths or the wavenumbers of the dissociation laser.

For the ultraviolet photodissociation experiment, we use a XeCl excimer laser (Lambda Physik LPX 105i) pumped dye laser (Lambda Physik LPD 3002) with an autotracker system (INRAD Autotracker II). The output of the dye laser is frequency-doubled through a BBO (β -BaB₂O₄) crystal placed on the autotracker system. A tunable infrared source is a commercial optical parametric oscillator (OPO) system (Continuum Mirage 3000) pumped with an injection-seeded Nd:YAG laser (Continuum Powerlite 9010). The output energies used in this work are kept in the range of 1–2 mJ/pulse and the linewidth is approximately 0.02 cm⁻¹. In all of the experiments, we carefully verify the proportion of the fragment yields to the laser power and control it to avoid the saturation effect. In the early stage of our infrared researches, we used a PbSe infrared detector as a laser power monitor.⁷ However, it was not suitable for the accurate normalization because the sensitivity of the PbSe detector is highly dependent on the wavelengths. By using the pyroelectric detector, whose sensitivity is independent of the wavelengths, we obtain more reliable infrared photodissociation spectra now.

III. RESULTS

Figure 1 displays the photodissociation spectra of (a) $(\text{C}_6\text{H}_6\bullet\text{Ar})^+$, (b) $(\text{C}_6\text{H}_6)_2^+$, and (c) $(\text{C}_6\text{H}_6)_3^+$ in the ultraviolet region (220–340 nm). C_6H_6^+ is detected as a photodissociation product for all species. The spectrum of $(\text{C}_6\text{H}_6\bullet\text{Ar})^+$ exhibits a broad band at 235 nm. The spectrum of $(\text{C}_6\text{H}_6)_2^+$ shows a tail of a VUV absorption band in the region from 220 to 260 nm. With our detection system, any noticeable band is not seen in the region from 260 to 340 nm for the dimer ion. The spectrum of $(\text{C}_6\text{H}_6)_3^+$ also shows a similar absorption tail from 220 nm to the red in addition to a broad band at 255 nm.

Figure 2 shows the photodissociation spectra of $(\text{C}_6\text{H}_6)_2^+$ in the 2500–12000 cm^{-1} region. The photodissociation spectrum in the near-infrared region (Fig. 2(a)) was measured previously by our group.¹ Two maxima are seen at 10930 cm^{-1} and 8660 cm^{-1} . These bands are assigned to the charge resonance bands of a dimer ion with a displaced sandwich structure.⁸ The charge resonance bands show very broad feature due to the transition to the repulsive state.¹ The intensity gradually decreases from 8660 cm^{-1} to the lower frequencies. Figure 2(b) shows the photodissociation spectrum of $(\text{C}_6\text{H}_6)_2^+$ in the infrared region. The spectrum shows the gradual decrease of the cross sections from 7000 to 3200 cm^{-1} , indicating that the tail of the charge resonance band extends down to the lower infrared region. In the region from 3200 to 2500 cm^{-1} , we can find two maxima at 2880 and 2670 cm^{-1} . Figure 2(c) represents a schematic diagram of the charge resonance states and the charge resonance transitions.

Photodissociation spectra of $(\text{C}_6\text{H}_6)_n^+$ ($n=2-5$) in the C–H stretching

(3000–3150 cm^{-1}) region are displayed in Fig. 3 (open circles). Photodissociation cross sections of $(\text{C}_6\text{H}_6)_n^+$ ($n=2-5$) are not zero from 3000 to 3150 cm^{-1} . The spectrum of $(\text{C}_6\text{H}_6)_2^+$ shows a sudden step at 3100 cm^{-1} with increasing intensity to the lower frequencies. The spectra of $(\text{C}_6\text{H}_6)_n^+$ ($n=3-5$) exhibit resolved bands centered at 3066 cm^{-1} . The spectrum of the trimer ion shows wings on both sides of the strongest band. In the spectra of the tetramer and the pentamer, we can find two bands at 3045 and 3093 cm^{-1} . The intensity ratios of these bands relative to the central band at 3066 cm^{-1} increase with increasing cluster size from the trimer to the pentamer. The band structure is overlapped with the plateau background signals. The plateau is shown in Fig. 3 by a thin horizontal line. Thick solid curves are the spectra synthesized from the components shown by the dotted curves. The method of analysis is given in a later section.

Figure 4 shows the laser power dependence of the yields of C_6H_6^+ emerging upon the photodissociation of $(\text{C}_6\text{H}_6)_2^+$ at 2900 cm^{-1} (open circles). The slope of the least square fitting (solid line) is 1.0 ± 0.1 , indicating that $(\text{C}_6\text{H}_6)_2^+$ is photodissociated by one-photon absorption of the infrared light. From an energetical point of view, this result seems somewhat counter-intuitive. The photon energy is only 0.36 eV (2900 cm^{-1}) although the binding energy of $(\text{C}_6\text{H}_6)_2^+$ is 0.67 eV.⁹ If the absorption occurs in the vibrational ground state, at least two photons are required to dissociate $(\text{C}_6\text{H}_6)_2^+$. Therefore, the absorption of $(\text{C}_6\text{H}_6)_2^+$ in the infrared region is attributed to hot band excitation from excited vibrational levels.

The photodissociation spectra of the mixed benzene dimer ion $(\text{C}_6\text{H}_6 \bullet \text{C}_6\text{D}_6)^+$ in

the C–H stretching region is shown in Fig. 5. To generate these spectra the ion yield for either $C_6H_6^+$ (solid curve) or $C_6D_6^+$ (dotted curve) is monitored while the OPO is scanned in the region 3000–3150 cm^{-1} . Both fragment ions of $C_6H_6^+$ and $C_6D_6^+$ exhibit similar excitation spectra. We note that the scanned region coincides with the C–H stretching region of the C_6H_6 moiety; the C_6D_6 C–D stretches lie lower in energy. Note also that the difference in ionization potential (IP) between C_6H_6 and C_6D_6 is only 0.003 eV.¹⁰ The evidence suggests that the positive charge is delocalized in $(C_6H_6 \bullet C_6D_6)^+$ because of the charge resonance interaction. The spectra are similar to the photodissociation spectrum observed for $(C_6H_6)_2^+$ (Fig. 3a), i.e. an absorption edge around 3080 cm^{-1} (perhaps a weak maximum), followed by a higher plateau on the lower frequency side. This band may be assigned tentatively to C–H stretching vibrations of C_6H_6 in $(C_6H_6 \bullet C_6D_6)^+$.

Figure 6 shows the infrared photodissociation spectra of the mixed benzene trimer ions that contain one or two benzene- d_6 molecules. The measured spectra are displayed as open circles. The solid lines are curve fits as discussed below. Photodissociation of benzene trimer ions with 3000–3150 cm^{-1} infrared light produces fragment dimer ions. In the photodissociation of $[(C_6H_6)_2 \bullet C_6D_6]^+$, the products $(C_6H_6 \bullet C_6D_6)^+$ and $(C_6H_6)_2^+$ are detected as the fragment ions. The photodissociation of $[C_6H_6 \bullet (C_6D_6)_2]^+$ produces $(C_6H_6 \bullet C_6D_6)^+$ or $(C_6D_6)_2^+$. The photodissociation spectra of the mixed benzene trimer ions are measured by detecting the respective fragment ions. All the spectra in Fig. 6 show peaks at 3066 cm^{-1} . The spectra of $[(C_6H_6)_2 \bullet C_6D_6]^+$ obtained by detecting $(C_6H_6 \bullet C_6D_6)^+$ and $(C_6H_6)_2^+$ (Fig. 6(a) and 6(b)) display close

similarity. The situation is the same for $[\text{C}_6\text{H}_6\bullet(\text{C}_6\text{D}_6)_2]^+$; the spectra (Fig. 6(c) and 6(d)) taken by detecting $(\text{C}_6\text{H}_6\bullet\text{C}_6\text{D}_6)^+$ and $(\text{C}_6\text{D}_6)_2^+$, respectively also display close similarity and in addition, are similar to the spectra displayed in Fig. 6(a) and 6(b). One may therefore conclude that the photodissociation spectra for the mixed trimers in the $3000\text{--}3150\text{ cm}^{-1}$ region do not depend on the monitored fragment ions. It may therefore be concluded that the photodissociation spectra of the mixed benzene trimer ions are essentially identical and moreover, they are indistinguishable from observations for that of the $(\text{C}_6\text{H}_6)_3^+$ trimer ion.

IV. DISCUSSION

A. Electronic spectrum of $(\text{C}_6\text{H}_6)_3^+$ in the ultraviolet region

On the basis of the photodissociation spectroscopy of $(\text{C}_6\text{H}_6)_3^+$ in the near-infrared region, we proposed that $(\text{C}_6\text{H}_6)_3^+$ has a dimer ion core structure with a neutral benzene attached: $(\text{C}_6\text{H}_6)_2^+\bullet\bullet\text{C}_6\text{H}_6$.^{2, 11} This structure is also supported by the ultraviolet photodissociation spectra shown in Fig. 1.

In the ultraviolet region, neutral benzene exhibits the well-known ${}^1B_{2u} \leftarrow {}^1A_{1g}$ (π, π^*) transition to the lowest excited singlet state (S_1). This $S_1 \leftarrow S_0$ transition of benzene appears around 260 nm with well-resolved vibronic structure.¹² The second excited singlet state (S_2) is ${}^1B_{1u}$ (π, π^*). The $S_2 \leftarrow S_0$ transition lies in the region from 204 nm to shorter wavelengths.¹³ It is expected that benzene ion also has a $\pi^* \leftarrow \pi$ transition in the ultraviolet region.^{14, 15} The $\pi^* \leftarrow \pi$ transition of benzene ion (${}^2E_{2u} \leftarrow {}^2E_{1g}$) is dipole-allowed for D_{6h} symmetry. Teng and Dunbar assigned the ultraviolet bands around 270 nm in the photodissociation spectra of substituted benzene ions to the $\pi^* \leftarrow \pi$ transitions.^{14, 15} On the same basis, we assign the band at 235 nm in Fig. 1(a) to the $\pi^* \leftarrow \pi$ transition of $(\text{C}_6\text{H}_6 \bullet \text{Ar})^+$. Since the IP of the Ar atom (15.759 eV)¹⁶ is much higher than that of benzene (9.243841 eV),¹⁰ the positive charge is localized in the benzene site, as expressed $\text{C}_6\text{H}_6^+ \bullet \bullet \bullet \text{Ar}$. Fujii and co-workers reported that an Ar atom in the $(\text{phenol})^+ \bullet \bullet \bullet \text{Ar}$ complex induces little perturbation to $(\text{phenol})^+$.^{17, 18} By analogy we assume that the perturbation by the Ar atom to the benzene ion is also not appreciable in the $\text{C}_6\text{H}_6^+ \bullet \bullet \bullet \text{Ar}$ complex. Therefore, we may attribute the band at 235 nm in the spectrum of $(\text{C}_6\text{H}_6 \bullet \text{Ar})^+$ to the $\pi^* \leftarrow \pi$ transition of C_6H_6^+ .

In the photodissociation spectrum of $(\text{C}_6\text{H}_6)_2^+$, the transitions to the two (π, π^*) states correlating to $\text{C}_6\text{H}_6^+(\pi, \pi^*)+\text{C}_6\text{H}_6(\text{S}_0)$ and $\text{C}_6\text{H}_6^+(\text{D}_0)+\text{C}_6\text{H}_6(\pi, \pi^*)$ must be observed in the ultraviolet region. Here D_0 denotes the ground doublet state of the ion. As seen in Fig. 1(b), however, we can only see the absorption tail of the VUV band at the wavelengths shorter than 240 nm. Tentatively, we assign this band to the $\pi^* \leftarrow \pi$ transition of $(\text{C}_6\text{H}_6)_2^+$.

The $(\text{C}_6\text{H}_6)_3^+$ cation with the dimer ion core structure is expected to show $\pi^* \leftarrow \pi$ transitions of both $(\text{C}_6\text{H}_6)_2^+$ and C_6H_6 chromophores in the ultraviolet region. The spectral feature of $(\text{C}_6\text{H}_6)_3^+$ in 220–240 nm is similar to that of $(\text{C}_6\text{H}_6)_2^+$; the absorption tail is seen at wavelengths shorter than 240 nm. Therefore, we assign this band to the $\pi^* \leftarrow \pi$ transition of the $(\text{C}_6\text{H}_6)_2^+$ chromophore. In addition to the tail, a broad band appears around 255 nm. Recognizing that the $\pi^* \leftarrow \pi$ transition in neutral benzene appears around 260 nm, we attribute the band at 255 nm to the $\pi^* \leftarrow \pi$ transition of the solvent C_6H_6 molecule. Thus the ultraviolet spectrum of $(\text{C}_6\text{H}_6)_3^+$ is consistent with the proposal that there is a dimer ion core associated with a neutral benzene ‘solvent’ molecule.

B. Assignment of infrared photodissociation spectra

In the spectra of $(\text{C}_6\text{H}_6)_n^+$ ($n=3-5$) shown in Fig. 3, we can see an intensity increase with increasing cluster size of the two subsidiary bands at 3045 and 3093 cm^{-1} relative to the central band at 3066 cm^{-1} . This intensity enhancement is thought to correspond to the increase in the number of neutral solvent molecules in the cluster ions.

Neutral benzene monomers are known to show three bands at 3048, 3079, and 3101 cm^{-1} in the C–H stretching region.¹⁹ Here we shall call them the C–H triad.¹⁹ We have attempted to reproduce the band shapes of $(\text{C}_6\text{H}_6)_n^+$ ($n=3-5$) by decomposing the spectra into three components: the triad, one Lorentzian function, and the plateau extending over this region. The relative intensities of the triad members used in the fit are taken from the measurement for neutral benzene clusters.²⁰ The triad and the Lorentzian components are shown by the dotted curves in Fig. 3. The plateau is drawn by the thin horizontal line. The thick solid curve represents the composition of the three components. It is clear that the thick solid curves well reproduce the observed band shapes. The ratios of the integrated intensity of the triad component to that of the Lorentzian component are 0.3, 0.6, and 0.9 for the trimer, tetramer, and pentamer, respectively. The ratio increases proportional to the number of the solvent benzene molecules in the clusters: 1, 2, and 3 neutral solvent molecules exist in the trimer, the tetramer, and the pentamer, respectively. Therefore, the Lorentzian component at 3066 cm^{-1} is assigned to the C–H stretching vibration of the dimer ion core. Now we can elucidate the infrared spectra of $(\text{C}_6\text{H}_6)_n^+$ ($n=3-5$) as the composites of the C–H stretching bands of the dimer ion core and the solvent benzene molecules. We discuss the plateau component later.

Neutral benzene has only one infrared-active C–H stretching mode, ν_{20} .¹⁹ The appearance of the triad in the infrared spectrum of the neutral benzene was thus attributed to the Fermi resonance interaction of the two combination modes with ν_{20} .¹⁹ In the case of $(\text{C}_6\text{H}_6)_2^+$, because of the vibrational frequency change due to the formation

of the dimer ion, the frequency gap between the infrared-active mode and the combination modes becomes larger, deactivating the Fermi resonance interaction. Thus, the original single band can appear as the C–H stretching vibration of the dimer ion core. The nice fitting of the experimental points with the composite curves in Fig. 3 implies that the intramolecular vibrational structure of the solvent benzene molecules in the clusters is not largely different from that of the isolated neutral benzene.

The infrared spectrum of the dimer ion in Fig. 3(a) shows the stepwise intensity change at 3100 cm^{-1} . According to the similarity in its position with the C–H stretching band of the dimer ion core of $(\text{C}_6\text{H}_6)_n^+$ ($n=3-5$), the stepwise increase may be attributed to the appearance of the C–H stretching band of $(\text{C}_6\text{H}_6)_2^+$. This assignment is also supported by the spectra of $(\text{C}_6\text{H}_6\bullet\text{C}_6\text{D}_6)^+$ shown in Fig. 5. However, we cannot determine the precise frequency due to the less-resolved band shape. The infrared spectrum of $(\text{C}_6\text{H}_6)_2^+$ in Fig. 2(b) also shows two maxima at 2670 and 2880 cm^{-1} . These bands might be assigned to some vibrational transitions of the hot species. The origin of these bands are not clear at the present stage.

C. Origin of plateau components observed in infrared photodissociation spectra

Let us think of the plateau component. As mentioned above, $(\text{C}_6\text{H}_6)_n^+$ ($n=2-5$) show the strong charge resonance band in the near-infrared region.² Since the charge resonance band corresponds to the transition to the repulsive excited state, the band shape is essentially broad.¹ As displayed in Fig. 2, the charge resonance bands of $(\text{C}_6\text{H}_6)_2^+$ display maxima at 10930 and 8660 cm^{-1} , and the intensity gradually decreases

from 8660 cm^{-1} to lower frequencies. Its tail extends down to 2500 cm^{-1} over the threshold of the binding energy of 5400 cm^{-1} (0.67eV). If the intermolecular stretching vibration of the sandwich dimer species is highly excited, the charge resonance transition is expected to appear even in the infrared region (see Fig. 2(c)). Consequently, the hot bands of the charge resonance transition may mainly contribute to the plateau component of the infrared spectra. This situation is in accord with the result of the laser power dependence of the photodissociation for $(\text{C}_6\text{H}_6)_2^+$ (Fig. 4).

Contribution of the charge resonance transition from vibrationally highly excited species to the plateau component is also recognized by comparing the infrared spectra of $(\text{C}_6\text{H}_6)_n^+$ ($n=2-5$) with each other (Fig. 3). The energy needed to dissociate a benzene molecule away from the parent cluster ions (binding energy) becomes lower and lower as the cluster size increases; the reported binding energies are 0.67 , 0.27 , 0.15 , and 0.13 eV for $n=2$, 3 , 4 , and 5 , respectively.⁹ Internal energies are expected to be smaller for the cluster ions with smaller binding energies. Therefore, the benzene cluster ions can get cooler and cooler with increasing cluster size. This trend was confirmed by our previous study on the unimolecular dissociation kinetics of the benzene cluster ions.⁵ As can be seen in Fig. 3, the intensity of the plateau component decreases for larger clusters. The ratios of the plateau components to the total cross sections at 3066 cm^{-1} are 0.30 , 0.20 , and 0.13 for $n=3$, 4 , and 5 , respectively. Since the decrease in the intensity of the plateau component coincides with the decrease in the internal energy for larger clusters, the main origin of the plateau component is attributed to the hot band excitation.

D. Dimer ion core switching in vibrational excited states of mixed benzene trimer ions

Figure 7 displays the relationship between the expected photoabsorption spectra of the respective isomers and the photodissociation spectra obtained in the C–H stretching region. According to small difference (0.003 eV) in IP, C_6H_6 and C_6D_6 behave as if these are equivalent molecules in the electronic and geometric structures of the trimer ions, although they show different vibrational frequencies.¹⁰ On the basis of our spectroscopic studies of $(C_6H_6)_3^+$, it is reasonable that the mixed benzene trimer ions also have the dimer ion core structure.

In the case of $[(C_6H_6)_2 \bullet C_6D_6]^+$, there are two possible isomers. One isomer is $(C_6H_6)_2^+ \bullet \bullet \bullet C_6D_6$, and the other is $(C_6H_6 \bullet C_6D_6)^+ \bullet \bullet \bullet C_6H_6$. For the former isomer one can expect that the photoabsorption spectrum shows a single Lorentzian band feature of the C–H stretching vibration of the $(C_6H_6)_2^+$ ion core. For the latter isomer, the photoabsorption spectrum is expected to be composed of a single Lorentzian band of the $(C_6H_6 \bullet C_6D_6)^+$ ion core and a triad of the solvent C_6H_6 . Let us suppose that the photoexcitation induces the cleavage of the weakest intermolecular bond after the intracluster vibrational energy redistribution *without* changing the position of the positive charge. We call this a frozen core model. In this model, the resultant fragment ion is the same as the dimer ion core in the ground state. For example, the fragment dimer ion produced by the photodissociation of $(C_6H_6)_2^+ \bullet \bullet \bullet C_6D_6$ is $(C_6H_6)_2^+$. Therefore, this model predicts spectral features for the photodissociation spectra with

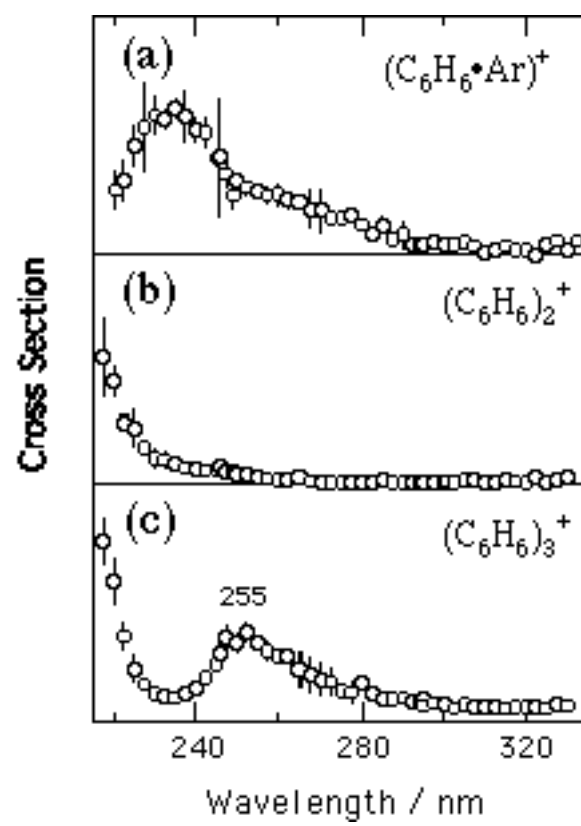
the respective fragment dimers. Those are shown in the fourth row of Fig. 7. Here the Lorentzian component represents the band feature of one C_6H_6 molecule existing in the dimer ion core. The triad component represents the band feature of a C_6H_6 molecule in the solvent part. The photodissociation spectrum of $[(C_6H_6)_2 \bullet C_6D_6]^+$ recorded with detecting $(C_6H_6)_2^+$ must exhibit one Lorentzian band of the dimer ion core, because each of two C_6H_6 molecules in the ion core shows the same Lorentzian band feature. The photodissociation spectrum recorded with detecting $(C_6H_6 \bullet C_6D_6)^+$ must show the composite feature of the ion core part and the solvent part. Photodissociation spectra detected with the respective fragment ions in Fig. 6(a) and 6(b), however, are nearly the same with each other. Therefore, the frozen core model does not agree with the observation. The observation can be explained reasonably with the following model. The discrepancy between the expected and the observed photodissociation spectra is due to the loss of the information on the photoexcited chromophore in the course of the dissociation. As shown in the fifth row of Fig. 7, the statistical abundance ratio of $(C_6H_6)_2^+ \bullet \bullet \bullet C_6D_6$ to $(C_6H_6 \bullet C_6D_6)^+ \bullet \bullet \bullet C_6H_6$ is 1:2. If we construct the two spectra of these isomers with this ratio, we obtain an overall photoabsorption spectrum of $[(C_6H_6)_2 \bullet C_6D_6]^+$ with the same feature as that of $(C_6H_6)_3^+$.²¹ If the photoexcited $[(C_6H_6)_2 \bullet C_6D_6]^+$ ejects a neutral benzene molecule after experiencing the frequent dimer ion core switching, the photodissociation spectrum observed through monitoring $(C_6H_6)_2^+$ becomes to be the same as that of $(C_6H_6 \bullet C_6D_6)^+$. In addition, the photodissociation spectra have the same feature as that of $(C_6H_6)_3^+$.

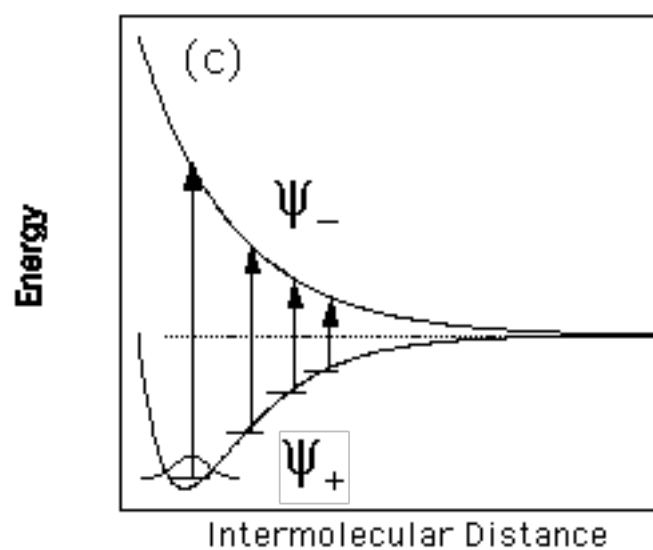
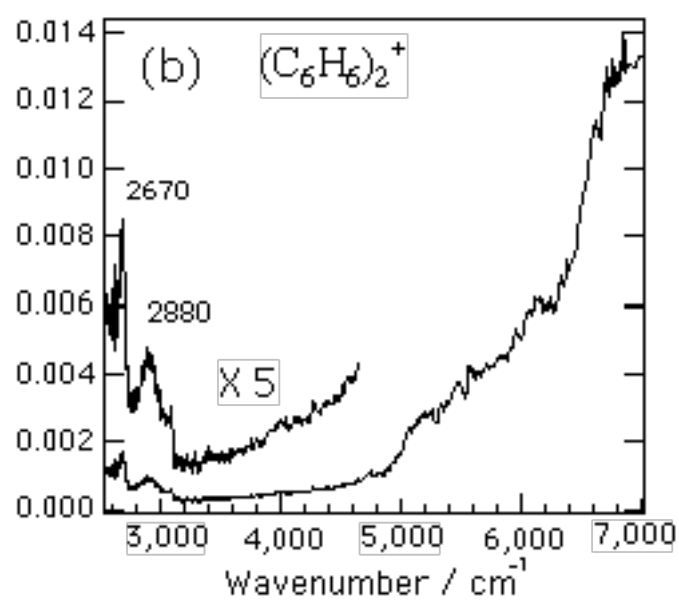
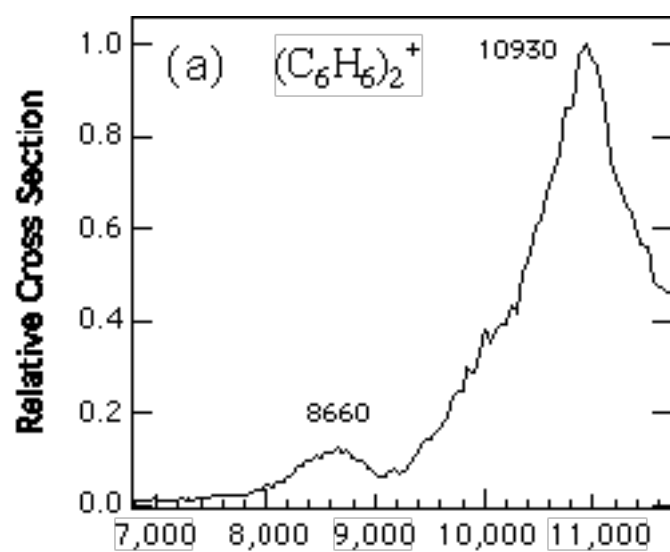
The same discussion can be applied to the case of $[C_6H_6 \bullet (C_6D_6)_2]^+$. The

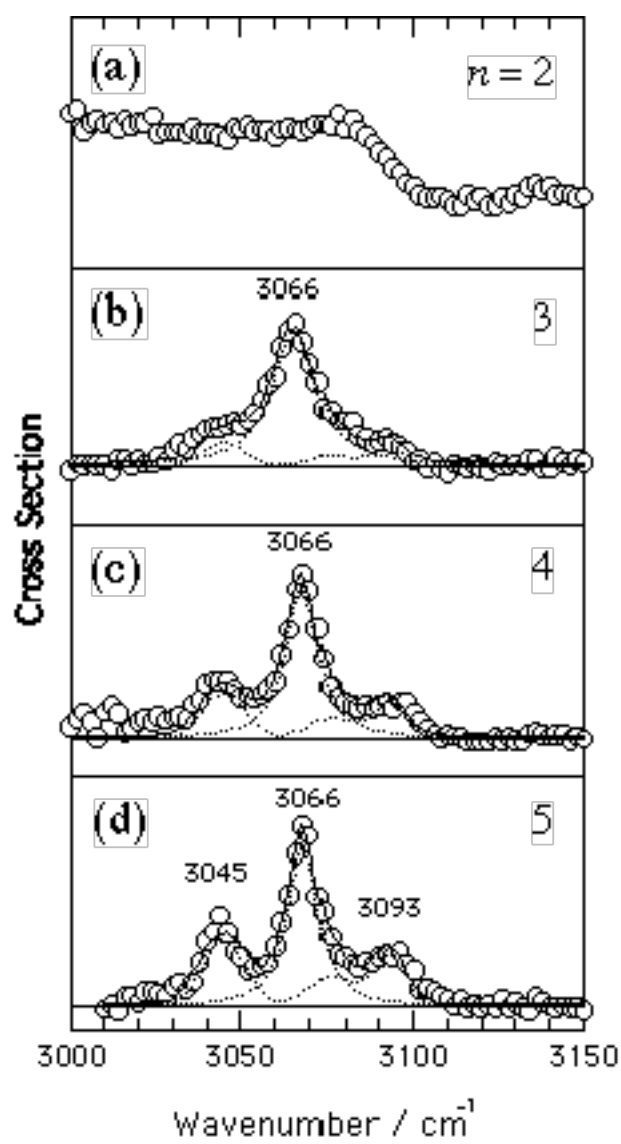
possible isomers are $(\text{C}_6\text{H}_6\bullet\text{C}_6\text{D}_6)^+\bullet\bullet\bullet\text{C}_6\text{D}_6$ and $(\text{C}_6\text{D}_6)_2^+\bullet\bullet\bullet\text{C}_6\text{H}_6$. The frozen core model predicts for the former isomer that the fragment ion is $(\text{C}_6\text{H}_6\bullet\text{C}_6\text{D}_6)^+$, and that the photodissociation spectrum shows a single Lorentzian band of the C–H stretching vibration of the $(\text{C}_6\text{H}_6\bullet\text{C}_6\text{D}_6)^+$ ion core. For the latter one, the model also predicts that the fragment ion is $(\text{C}_6\text{D}_6)_2^+$, and that the photodissociation spectrum shows the C–H stretching Fermi triad of the solvent C_6H_6 . Thus the frozen core model predicts different photodissociation spectra for monitoring the respective fragment ions. However, the observation is not the case: the spectrum in Fig. 6(c) is very similar to that in Fig. 6(d), and also similar to that of $(\text{C}_6\text{H}_6)_3^+$. The statistical mixing of the two spectra produces an overall photoabsorption spectrum of $[\text{C}_6\text{H}_6\bullet(\text{C}_6\text{D}_6)_2]^+$ identical to that of $(\text{C}_6\text{H}_6)_3^+$. Therefore, if the dissociation occurs after the frequent dimer ion core switching in the photoexcited state, the spectrum obtained through detecting $(\text{C}_6\text{H}_6\bullet\text{C}_6\text{D}_6)^+$ becomes to be identical to that of $(\text{C}_6\text{D}_6)_2^+$. In addition, these photodissociation spectra are almost the same as that of $(\text{C}_6\text{H}_6)_3^+$. Thus our data suggest that the dimer ion core switching, in other words, the charge hopping occurs in the photoexcited vibrational states of benzene trimer ions prior to the dissociation. From the linewidth of the Lorentzian components, the fastest limit of the hopping rate is estimated to be 2 ps.

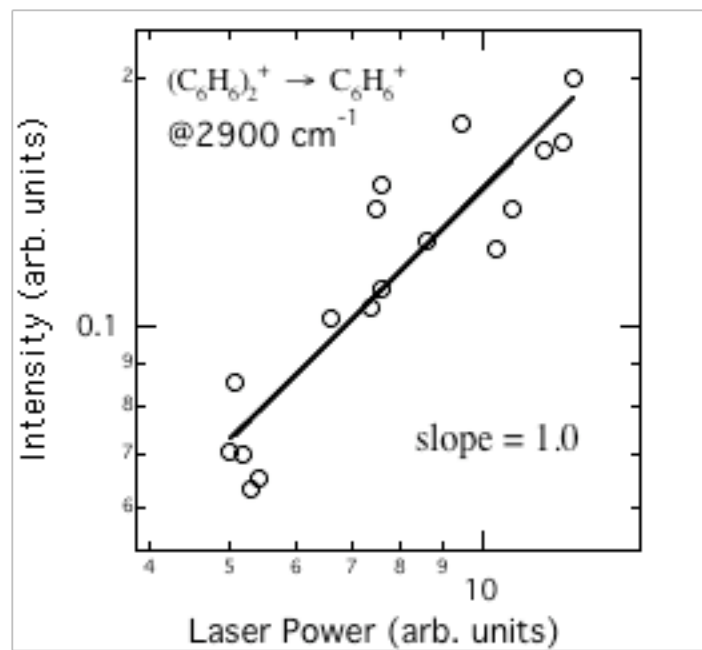
V. CONCLUSION

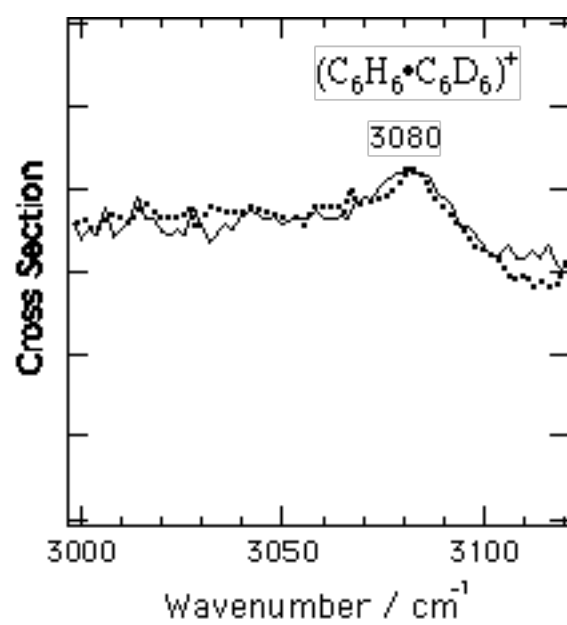
The photodissociation spectra of benzene cluster ions are measured in both ultraviolet and infrared regions. In particular we pay our attention to the trimer ions. The spectra provide information on static and dynamic behavior of the positive charge existing in the benzene trimer ions. In the ultraviolet photodissociation spectrum of $(\text{C}_6\text{H}_6)_3^+$, the $\pi^* \leftarrow \pi$ transition at 255 nm is assigned due to the solvent C_6H_6 . We can also reasonably explain the infrared spectrum of $(\text{C}_6\text{H}_6)_3^+$ by the dimer ion core model; the C–H stretching band of $(\text{C}_6\text{H}_6)_3^+$ is composed of the C–H stretching bands of the dimer ion core and the solvent benzene. On the other hand, the infrared spectra of the isotopically mixed benzene trimer ions show that the positive charge frequently hops from one dimer pair to another pair in the photoexcited vibrational states in the course of the dissociation.











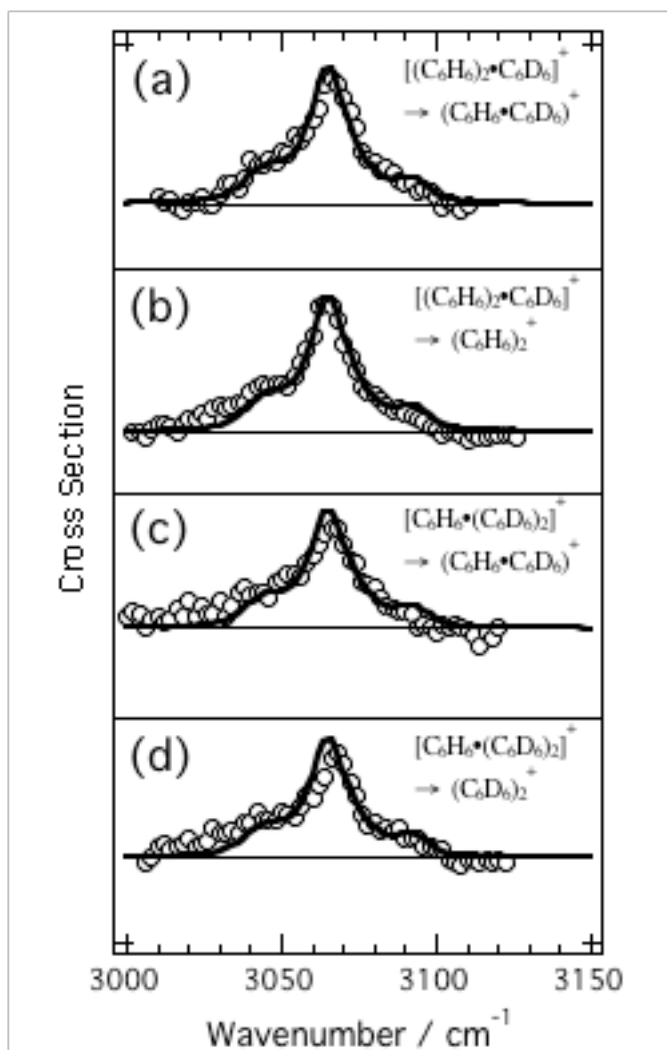


FIG. 6. Inokuchi,
The Journal of Chemical Physics

Species	$(C_2H_2)^+$	$[(C_2H_2)_2 \cdot C_2D_2]^+$		$[C_2H_2 \cdot (C_2D_2)_2]^+$	
Isomers	$(C_2H_2)^+ \leftrightarrow C_2H_2^+$	$(C_2H_2)^+ \leftrightarrow C_2D_2^+$	$(C_2H_2 \cdot C_2D_2)^+ \leftrightarrow C_2H_2^+$	$(C_2H_2 \cdot C_2D_2)^+ \leftrightarrow C_2D_2^+$	$(C_2D_2)^+ \leftrightarrow C_2H_2^+$
Ion core	$(C_2H_2)^+$	$(C_2H_2)^+$	$(C_2H_2 \cdot C_2D_2)^+$	$(C_2H_2 \cdot C_2D_2)^+$	$(C_2D_2)^+$
Spectral feature expected for frozen core model	 + + 	 + 	 + 		
Statistical abundance ratio	—	1 : 2		2 : 1	
Statistically mixed spectra	—				
Observed spectral feature					

REFERENCES AND NOTE

- ¹ K. Ohashi, Y. Nakai, T. Shibata, and N. Nishi, *Laser Chem.* **14**, 3 (1994).
- ² Y. Nakai, K. Ohashi, and N. Nishi, *J. Phys. Chem. A* **101**, 472 (1997).
- ³ K. Ohashi and N. Nishi, *J. Chem. Phys.* **109**, 3971 (1998).
- ⁴ M. Matsumoto, Y. Inokuchi, K. Ohashi, and N. Nishi, *J. Phys. Chem. A* **101**, 4574 (1997).
- ⁵ K. Ohashi, K. Adachi, and N. Nishi, *Bull. Chem. Soc. Jpn.* **69**, 915 (1996).
- ⁶ J. W. Farley, *Rev. Sci. Instrum.* **56**, 1834 (1985).
- ⁷ Y. Inokuchi, K. Ohashi, and N. Nishi, *Chem. Phys. Lett.* **279**, 73 (1997).
- ⁸ K. Ohashi, Y. Inokuchi, and N. Nishi, *Chem. Phys. Lett.* **263**, 167 (1996).
- ⁹ B. Ernstberger, H. Krause, and H. J. Neusser, *Ber. Bunsenges. Phys. Chem.* **97**, 884 (1993).
- ¹⁰ R. G. Neuhauser, K. Siglow, and H. J. Neusser, *J. Chem. Phys.* **106**, 896 (1997).
- ¹¹ T. Shibata, K. Ohashi, Y. Nakai, and N. Nishi, *Chem. Phys. Lett.* **229**, 604 (1994).
- ¹² G. H. Atkinson and C. S. Parmenter, *J. Mol. Spectrosc.* **73**, 52 (1978).
- ¹³ A. Hiraya and K. Shobatake, *Chem. Phys. Lett.* **178**, 543 (1991).
- ¹⁴ R. C. Dunbar, *J. Chem. Phys.* **68**, 3125 (1978).
- ¹⁵ H. H. Teng and R. C. Dunbar, *J. Chem. Phys.* **68**, 3133 (1978).
- ¹⁶ K. Kimura, S. Katsumata, Y. Achiba, T. Yamazaki, S. Iwata, in *Handbook of HeI Photoelectron Spectra of Fundamental Organic Molecules*, edited by K. Kimura (Japan Scientific Societies Press, Tokyo, 1981), p. 22.
- ¹⁷ A. Fujii, T. Sawamura, S. Tanabe, T. Ebata, and N. Mikami, *Chem. Phys. Lett.* **225**, 104 (1994).
- ¹⁸ A. Fujii, A. Iwasaki, T. Ebata, and N. Mikami, *J. Phys. Chem. A* **101**, 5963 (1997).
- ¹⁹ R. H. Page, Y. R. Shen, and Y. T. Lee, *J. Chem. Phys.* **88**, 5362 (1988).
- ²⁰ M. F. Vermon, J. M. Lisy, H. S. Kwok, D. J. Krajnovich, A. Tramer, Y. R. Shen, and Y. T. Lee, *J. Phys. Chem.* **85**, 3327 (1981).
- ²¹ In the case of $(C_6H_6)_3^+$, the band feature is reproduced by the composite of two Lorentzian and one triad components (see in the fourth row of Fig. 7). For the overall absorption spectrum of $[(C_6H_6)_2 \bullet C_6D_6]^+$, one must consider the composite of four Lorentzian and two triad components. Two of the four Lorentzian components are due

to $(\text{C}_6\text{H}_6)_2^+\cdots\text{C}_6\text{D}_6$. The rest of the Lorentzian components and the triad components are owing to the contribution from $(\text{C}_6\text{H}_6\cdots\text{C}_6\text{D}_6)^+\cdots\text{C}_6\text{H}_6$. (The relative abundance of the latter isomer is assumed to be twice of the former one.) Accordingly, the overall absorption spectrum of $[(\text{C}_6\text{H}_6)_2\cdots\text{C}_6\text{D}_6]^+$ has the same feature as the spectrum of $(\text{C}_6\text{H}_6)_3^+$.

FIGURE CAPTIONS

FIG. 1. Photodissociation spectra of (a) $(\text{C}_6\text{H}_6 \bullet \text{Ar})^+$, (b) $(\text{C}_6\text{H}_6)_2^+$, and (c) $(\text{C}_6\text{H}_6)_3^+$ in the ultraviolet region. The error bars indicate one standard deviation of statistical uncertainties determined by repeated laser scans.

FIG. 2. Photodissociation spectra of $(\text{C}_6\text{H}_6)_2^+$ in the 2500–12000 cm^{-1} region.

FIG. 3. Photodissociation spectra of $(\text{C}_6\text{H}_6)_n^+$ in the C–H stretching region (open circles). Figures 3(a)–3(d) correspond to the spectra of $n=2$ –5, respectively. Solid thick curves represent the results of the model fitting for the experimental points. Dotted curves and thin horizontal lines are the components used for the fittings (see text).

FIG. 4. Double logarithmic plots of the yields of C_6H_6^+ ions against the laser power for the photodissociation of $(\text{C}_6\text{H}_6)_2^+$ at 2900 cm^{-1} (open circles). The solid line represents the least-square fitting. The slope of the solid line is 1.0 ± 0.1 .

FIG. 5. Photodissociation spectra of $(\text{C}_6\text{H}_6 \bullet \text{C}_6\text{D}_6)^+$ in the C–H stretching region. The two spectra are measured by monitoring the yields of the fragment ions of C_6H_6^+ (solid curve) and C_6D_6^+ (dotted curve).

FIG. 6. Photodissociation spectra (open circles) of $[(C_6H_6)_2 \bullet C_6D_6]^+$ ((a) and (b)) and $[C_6H_6 \bullet (C_6D_6)_2]^+$ ((c) and (d)). The fragment ions monitored in the respective experiments are (a) $(C_6H_6 \bullet C_6D_6)^+$, (b) $(C_6H_6)_2^+$, (c) $(C_6H_6 \bullet C_6D_6)^+$, and (d) $(C_6D_6)_2^+$. The thick solid curves represent the fitting curve used for the spectrum of $(C_6H_6)_3^+$.

FIG. 7. Expected photoabsorption spectra of the isomers based on the frozen core model and the observed spectral feature in the C–H stretching region. The possible isomers are displayed in the second row. In the fifth row, the ratios of the isomer abundance in the statistical limit are shown. In the seventh row, we represent the band feature of the photodissociation spectra observed in this study.